

Published in final edited form as:

Cancer Res. 2009 April 1; 69(7): 3173–3179. doi:10.1158/0008-5472.CAN-08-3390.

Non-invasive imaging of $\alpha_v\beta_3$ function as a predictor of the anti-migratory and anti-proliferative effects of dasatinib

Rebecca A. Dumont¹, Isabel Hildebrandt¹, Helen Su¹, Roland Haubner², Gerald Reischl³, Johannes G. Czernin¹, Paul S. Mischel^{1,4}, and Wolfgang A. Weber⁵

¹Department of Molecular and Medical Pharmacology, David Geffen School of Medicine, University of California Los Angeles, Los Angeles, California

²Department of Nuclear Medicine, Medical University of Innsbruck, Innsbruck, Austria

³Division of Radiopharmacy, University Hospital of Tübingen, Tübingen, Germany

⁴Department of Pathology and Laboratory Medicine, David Geffen School of Medicine, University of California Los Angeles, Los Angeles, California

⁵Department of Nuclear Medicine, University of Freiburg, Freiburg, Germany

Abstract

Introduction—Src family kinases (SFK) are commonly deregulated in cancer cells. Among other functions SFK are critical for cellular migration and invasion. SFK inhibitors are being studied as targeted cancer drugs, but there are no biomarkers for non-invasive assessment of SFK inhibition. The aim of this study was to evaluate whether imaging of $\alpha_v\beta_3$ integrin activity with PET and [⁶⁴Cu]DOTA–cyclo-Arg-Gly-Asp-Phe-Lys ([⁶⁴Cu]DOTA–c(RGDfK)) can be used for monitoring response to the SFK inhibitor dasatinib.

Methods—SCID mice bearing U87MG xenografts were gavaged daily over 72 hours with 72 or 95 mg/kg dasatinib, or vehicle. Tumor uptake of [⁶⁴Cu]DOTA–c(RGDfK) was measured by small animal PET. In parallel, fluorodeoxyglucose (FDG) scans were performed to assess tumor metabolism in response to dasatinib treatment.

Results—Dasatinib significantly ($p < 0.0001$) reduced [⁶⁴Cu]DOTA–c(RGDfK) uptake by up to 59% in U87MG xenografts ($2.10 \pm 0.14\%$ ID/g in the 95 mg/kg group, $3.12 \pm 0.18\%$ ID/g in the 72 mg/kg group, versus $5.08 \pm 0.80\%$ ID/g in controls). In contrast, tumor FDG uptake showed no significant reduction with dasatinib therapy ($8.13 \pm 0.45\%$ ID/g in treated vs $10.39 \pm 1.04\%$ ID/g in controls, $p = 0.170$). Histologically, tumors were viable at the time of the follow-up PET scan, but showed inhibition of focal adhesion kinase. Continued dasatinib treatment resulted in a significant inhibition of tumor growth (tumor size on day 10 of therapy 21.13 ± 2.60 mm² in treated animals vs 122.50 ± 17.68 mm² in controls, $p = 0.001$).

Conclusions—[⁶⁴Cu]DOTA–c(RGDfK) may provide a sensitive means of monitoring tumor response to SFK inhibition in $\alpha_v\beta_3$ expressing cancers early in the course of therapy.

Keywords

RGD peptide; $\alpha_v\beta_3$; PET imaging; dasatinib

For correspondence or reprints: Rebecca A. Dumont, Department of Molecular and Medical Pharmacology, David Geffen School of Medicine at UCLA, 26-059 CHS, 10833 Le Conte Ave, Los Angeles, CA 90095-6948, Telephone: (310) 206-7008, Email: rdumont@ucla.edu.

Conflicts of interest: none

INTRODUCTION

Molecularly targeted therapies are becoming increasingly important in the treatment of cancer as the signaling mechanisms underlying malignancy are elucidated. While some small molecule inhibitors are effective in a large percentage of patients, as is the case with imatinib in the treatment of chronic myeloid leukemia, most targeted therapies are clinically effective in a limited subset of patients with common solid tumors (eg, erlotinib in non-small cell lung cancer¹). In addition, tumors that initially respond frequently proceed to develop resistance to targeted therapy. Therefore, identifying new therapeutic agents and a means by which to predict and monitor treatment response are compelling priorities in the field of oncology.

Inhibition of platelet derived growth factor receptor (PDGFr) and Src family kinases (SFK) is a promising anti-cancer strategy, as both oncogenes are known to be upregulated and important in the pathogenesis of various malignancies including glioblastoma multiforme (GBM), soft tissue sarcoma, gastrointestinal cancer, pancreatic cancer, and melanoma²⁻⁵. Preclinical studies have shown that inhibition of PDGFr can inhibit growth and reduce the invasiveness of tumor cells, effects that are mediated through activation of SFK^{6,7}. These studies support the clinical testing of dasatinib, an inhibitor of SFK (and other tyrosine kinases) in solid tumors, and clinical trials have recently started in glioblastoma, pancreatic adenocarcinoma, breast cancer, and non-small cell lung cancer, among others. Such trials would benefit from non-invasive techniques to monitor the molecular changes in response to dasatinib therapy.

Positron Emission Tomography (PET) is a valuable tool for identifying the molecular changes following therapeutic interventions in patients. For monitoring effects of SFK inhibitors in patients, PET probes binding to the $\alpha_v\beta_3$ integrin are of particular interest. The integrin $\alpha_v\beta_3$ is a cellular adhesion molecule that is frequently expressed on malignant tumors and acts as an important receptor affecting tumor growth, local invasiveness, and metastatic potential⁸. SFK activity is necessary for localization of $\alpha_v\beta_3$ to focal adhesions and integrin-mediated migration and invasion⁷.

For imaging of the $\alpha_v\beta_3$ integrin, cyclic pentapeptides containing the tripeptide sequence arginine-glycine-aspartate (RGD) have been developed. These peptides specifically bind to $\alpha_v\beta_3$ in its activated state, but not to related integrins such as $\alpha_{IIb}\beta_3$ ^{9,10}. Recent clinical trials have demonstrated that PET imaging with radiolabeled RGD peptides allows quantitative expression of activated $\alpha_v\beta_3$ integrin in patients with various malignant tumors^{10,11}.

Based on these data, we hypothesized that PET imaging with radiolabeled RGD peptides may provide a non-invasive readout for the anti-invasive effects of SFK inhibition. As a model to test this hypothesis we used U87MG, a GBM cell line with high expression of $\alpha_v\beta_3$ in which PDGFr inhibition has a significant anti-migratory effect in a SFK-dependent manner⁷. We show evidence that dasatinib alters invasion of glioblastoma cells and we demonstrate that the radiolabeled RGD peptide [⁶⁴Cu]DOTA-c(RGDfK) can be used to monitor treatment response to dasatinib *in-vivo*.

MATERIALS AND METHODS

Cell culture

The glioma cell line U87MG was purchased from the American Type Culture Collection (ATCC, Manassas, VA) and cultured in DMEM (Invitrogen, Carlsbad, CA) supplemented with 10% fetal bovine serum (Omega Scientific, Tarzana, CA), 2 mg/mL glucose, 100 units/mL of penicillin, and 100 units/mL of streptomycin (Invitrogen, Carlsbad, CA). Cells were grown at 37°C in an atmosphere of 5% CO₂.

Invasion assay

To assess the impact of dasatinib on cell motility, a two-dimensional invasion assay was performed using six-well Transwell polycarbonate membrane inserts with 8.0 μm pores (CoStar, Cambridge, MA) coated from the bottom with 25 $\mu\text{g}/\text{ml}$ fibronectin (Chemicon, Temecula, CA) as an extracellular matrix barrier. After adding serum-free MEM to the lower compartments, 5×10^5 U87MG cells in serum-free MEM/BSA (5 mg/ml) were seeded onto the upper chambers and incubated for 6 h at 37°C, 5% CO_2 . For pharmacological inhibition, dasatinib (Bristol-Myers Squibb Oncology, Princeton, NJ) or c(RGDfK) (Peptides International, Louisville, Kentucky) was added to cells in the upper chamber at the designated concentrations at the time of plating. DMSO was used as a vehicle control (VC) and to dilute the 20 mM stock dasatinib. After 6 hours, non-invasive cells on the upper surface were removed with cotton swabs, and the remaining invaded cells on the lower surface fixed in 4% paraformaldehyde and stained with 0.25% cresyl violet. The number of invasive cells was calculated using pictures of 6 random fields per filter taken with an Olympus BX61 microscope (Olympus, Center Valley, PA) at 40 \times magnification, then calculating the area in each photomicrograph with purple staining using Soft Imaging Software (Olympus).

Western blot analysis

Protein expression and phosphorylation were assessed by Western blotting of lysates from cells treated for 6 hours with 100 nM dasatinib or control. Antibodies were used against phospho-Src (Y416) (Cell Signaling, Boston, MA); phospho-FAK (Y397) (Abcam, Cambridge, MA); phospho-FAK (Y861) (Biosource-Invitrogen, Camarillo, CA); and actin (Sigma, St. Louis, MO). Lysates treated for 24 hours with 100 nM dasatinib or control were stained for β_3 expression (Chemicon, Temecula, CA) and actin (Sigma). Blotting was performed according to the manufacturer's instructions and imaged with the LI-COR Odyssey Imager using infrared dye-conjugated secondary antibodies (LI-COR, Lincoln, Nebraska).

Immunofluorescence

To assess focal contact formation, cells grown on 8-well fibronectin coated slides (BD BioCoat, Bedford, MA) and treated for 6 hours with 100 nM dasatinib were fixed in 4% paraformaldehyde-PBS at 37°C, permeabilized with 0.3% triton-PBS, and blocked overnight in 10% normal goat serum-PBS at 4°C. One microgram of the anti- $\alpha_v\beta_3$ antibody LM609 (Chemicon) was labeled with 10 μl of IgGTRIT-C primary labeling solution (Invitrogen) per manufacturer's instructions. DAPI (Invitrogen) was used as a nuclear stain, and slides were mounted with VECTASHIELD® (Vector Laboratories, Burlingame, CA) for imaging with an Olympus BX61 microscope.

Flow cytometry

U87MG surface $\alpha_v\beta_3$ integrin expression was analyzed following 6 and 24 hours of treatment with 100 nM dasatinib using the anti- $\alpha_v\beta_3$ antibody LM609 (Chemicon) and goat F(ab')₂ anti-mouse IgG-phycoerythrin (R&D Systems, Minneapolis, MN)¹². Samples were read on a FACScan Analytic Flow Cytometer (Becton Dickinson, Franklin Lakes, NJ).

Western blots, immunofluorescence and flow cytometry were performed after overnight incubation on pre-coated fibronectin tissue culture plates (BD BioCoat).

⁶⁴Cu labeling of DOTA-c(RGDfK)

The peptide DOTA-c(RGDfK) was synthesized as described previously¹³. Labeling with copper-64 chloride (MDS Nordion, Vancouver, BC, Canada) was performed by incubating 1.25 μg DOTA-c(RGDfK) with 37 MBq ⁶⁴Cu for 1 hour at 50°C in a total volume of 200 μl 0.1M Ammonium Acetate at pH 7.1. Purification of the radio-labeled peptide was performed

using a 1 mL Strata™-X 33 μm polymeric reversed phase column (Phenomenex, Inc, Torrance, CA). Following a water wash, the labeled peptide was eluted in 100% ethanol, dried over argon gas at 60°C and resuspended in 0.9% saline. All labeling solutions were pretreated with Chelex-100 (Bio-Rad, Hercules, CA) at 1.2 g/L. Labeling efficiency ranged from 75–85%, for a specific activity of the radiolabeled peptide of 22.2–25.6 GBq/mg. Thus the amount of peptide injected ranged between 0.74 and 0.83 μg .

Xenograft model and dasatinib treatment

Severe combined immunodeficient (*SCID*) mice were purchased from Jackson Lab (Bar Harbor, MN). All animal manipulations were performed with sterile technique following the guidelines of the UCLA Animal Research Committee. U87MG (2×10^6 cells/mouse) were resuspended in PBS and Matrigel (BD Biosciences, Bedford, MA), and injected subcutaneously at the right shoulder of 7 week old male mice. After tumors had grown to an approximate size of 6 mm, groups of 3–5 animals were gavaged daily with vehicle (1:1 propylene glycol: water), 72 mg/kg, or 95 mg/kg dasatinib. Tumor length and width were measured over a 10 day period with calipers.

Micro-PET/CT Imaging

Sixty minute dynamic microPET/CT scans were obtained with 15–20 MBq (peptide mass: 0.74–0.83 μg) [^{64}Cu]DOTA–c(RGDfK) injected via tail vein after 72 hours of dasatinib treatment using a micro-PET FOCUS 220 PET scanner (Siemens, Malvern, PA) and a MicroCAT II CT scanner (Siemens)¹⁴. Fifteen hours later, animals underwent another microPET/CT study (10 min static emission scan, 7 min microCT scan)^{15,16}. PET images were reconstructed by filtered back projection, using a ramp filter to yield an image resolution of 1.7 mm¹⁷. In a separate experiment, static emission [^{18}F]fluorodeoxyglucose (FDG) microPET/CT scans were performed with 7–10 MBq FDG (mass less than 0.1 μg) after 1 hour uptake in animals treated for 72 hours with dasatinib or vehicle control (VC).

Image analysis

To determine tracer concentration in various tissues, ellipsoid regions of interest (ROIs) were placed in the region that exhibited the highest radioactivity as determined by visual inspection on fused micro-PET/CT images generated by the AMIDE software¹⁸. Tracer uptake in the xenograft tumors and normal tissues are expressed as percent of the decay-corrected injected activity per cm³ of tissue (% ID/g). Previous studies have shown that uptake of [^{64}Cu]DOTA–c(RGDfK) correlates closely with the expression of activated $\alpha_V\beta_3$ integrins¹⁹.

Immunohistochemistry

Following anesthetization and sacrifice of mice, tumors were removed and frozen in liquid nitrogen. Frozen tumor tissues were sectioned (6 μm) and stained with hematoxylin and eosin (H&E) following standard protocols, or immunohistochemically stained with primary antibodies against CD31 (BD Pharmingen, San Jose, CA), phospho-FAK (Y861) (Biosource-Invitrogen), and $\alpha_V\beta_3$ (Chemicon), followed by biotinylated secondary antibodies and avidin-biotin complex (Vector Laboratories, Burlingame, CA). Visualization of all staining was performed with NovaRed substrate (Vector Laboratories) and tissues were counterstained with hematoxylin. Images were generated with an Olympus BX61 microscope.

Statistical analysis

Quantitative results are expressed as mean \pm 1 standard deviation (SD). Comparisons were made by t-tests or by analysis of variance (ANOVA) as appropriate (GraphPad Prism, GraphPad Software, San Diego, CA). Differences were considered significant when $p < 0.050$.

RESULTS

U87 invasion is dependent on $\alpha_V\beta_3$ function and is inhibited by dasatinib

U87MG cells plated in fibronectin-coated Boyden chambers and treated with 50 nM or 100 nM dasatinib for 6 hours showed a significant reduction in invasion compared to control ($40.30 \pm 7.86\%$ and $15.36 \pm 5.70\%$ of control, respectively, $p < 0.001$) (Figures 1A and B). To determine the importance of $\alpha_V\beta_3$ function in U87MG invasion, cells were treated with 2 mM c(RGDfK) peptide to effectively saturate all available functional binding sites²⁰. This inhibited the ability of U87MG to invade through fibronectin to $11.48 \pm 3.35\%$ of controls ($p < 0.001$) (Figures 1A and B). A similar reduction in invasiveness was observed when cells were grown on collagen, which is not a ligand of the $\alpha_V\beta_3$ integrin.

Dasatinib inhibits phosphorylation of Src family kinases and Focal Adhesion Kinase, and impairs the formation of focal adhesions

Cell lysates prepared for Western blot following 6 hours of 100 nM dasatinib treatment showed target inhibition of SFK phosphorylation at activation site tyrosine 416 and FAK at tyrosine 861 phosphorylation, a SFK-dependent activation site. A decrease was also seen in FAK tyrosine 397, an integrin-dependent autophosphorylation site (Figure 2A).

Immunofluorescence was used to study the impact of SFK/FAK inhibition on the formation of focal adhesion complexes in U87 cells on a fibronectin surface. Staining for dimerized $\alpha_V\beta_3$ showed the integrin localized on the cell surface in numerous focal adhesions in control U87MG cells (Figure 2B). Following 3 hours of 100 nM dasatinib treatment, cell morphology was notably altered as seen in the images and $\alpha_V\beta_3$ was no longer clustered in focal adhesion complexes (Figure 2B). By 6 hours, the ability of the cells to remain attached to the fibronectin surface was so impaired that there were insufficient numbers of attached cells remaining on the slides to stain. Total levels of dimerized cell surface $\alpha_V\beta_3$ protein level following 6 or 24 hours of 100 nM dasatinib did not change relative to control as assessed by FACS, nor did total β_3 levels decrease in a Western blot of corresponding cell lysates (Figure 2C and D, 6 hour data not shown).

Dasatinib decreases uptake of [⁶⁴Cu]DOTA–c(RGDfK) in U87MG xenografts and markedly inhibits tumor growth

Dasatinib treatment significantly reduced [⁶⁴Cu]DOTA–c(RGDfK) uptake by 39% in the 72 mg/kg dose group and 59% in the 95 mg/kg dose group after 72 hours of treatment ($2.10 \pm 0.14\%$ ID/g N=3 in 95 mg/kg, $3.12 \pm 0.18\%$ ID/g N=4 in 72 mg/kg, $5.08 \pm 0.80\%$ ID/g N=7 in controls) as shown in Figures 3A and B, ($p < 0.0001$, 1-way ANOVA). Tumor to muscle and tumor to blood ratios showed similar changes with dasatinib therapy (Figures 3C and D). The effect of dasatinib on tracer kinetics in the tumor and normal organs were examined with dynamic PET scans, which showed that tracer distribution and organ uptake were virtually identical between treated and untreated animals except in the U87 xenografts (Figure 4).

In contrast to the RGD peptide tracer, there was no significant change in FDG uptake with 72 hours of 95 mg/kg dasatinib treatment (Figure 5A, $p = 0.1704$) indicating that the tumor cells remained viable during dasatinib treatment.

U87MG tumor growth was markedly inhibited with continued dasatinib treatment, resulting in a six-fold difference in tumor size between control ($122.50 \pm 17.68 \text{ mm}^2$) and treated animals ($21.13 \pm 12.60 \text{ mm}^2$) after 10 consecutive days of treatment (t-test, $p = 0.0011$). However, at the time of PET imaging no appreciable difference in tumor size was present (Figure 5B, $p = 0.1272$).

Dasatinib does not decrease in-vivo tumor viability, vascularization or $\alpha_V\beta_3$ expression, while target inhibition is demonstrated

Target inhibition of the subcutaneous tumors was demonstrated by staining for phospho-FAK (Y861), which was reduced in treated tumors relative to control. Nevertheless, U87MG subcutaneous xenografts remained viable and vascularized following 72 hours of treatment with 95 mg/kg dasatinib as demonstrated by staining with H&E and the endothelial marker CD31 (Figure 5C). There was also no difference in $\alpha_V\beta_3$ staining between treated and control tumors (Figure 5C).

DISCUSSION

In this study we show that dasatinib treatment of human glioblastoma xenografts causes a rapid decrease in the uptake of the radiolabeled $\alpha_V\beta_3$ ligand [^{64}Cu]DOTA-c(RGDfK). In contrast, imaging of tumor glucose metabolism with FDG-PET did not reveal significant differences between animals treated with vehicle or dasatinib, although tumor growth was markedly inhibited by dasatinib therapy after ten days of treatment. These findings suggest that PET with [^{64}Cu]DOTA-c(RGDfK) may represent a useful biomarker for monitoring non-invasively the cytostatic effects of dasatinib therapy.

Others have previously reported that dasatinib inhibits *in-vitro* invasion in a variety of solid tumor types at nanomolar concentrations, confirming that invasion is commonly mediated through the activity of SFK in malignant cells^{21,22}. Our *in-vitro* data showing a significant loss of invasiveness after treatment with 50 nM dasatinib demonstrate that this is also the case in the U87MG glioma cell line. Furthermore, our *in-vitro* data indicate that U87MG relies heavily on the interaction between $\alpha_V\beta_3$ and specific substrates such as fibronectin for invasion in a 2-D invasion model. When integrin binding sites were saturated with an excess of c(RGDfK), or when $\alpha_V\beta_3$ binding substrate was absent as on a collagen surface, *in-vitro* invasion of U87MG cells was greatly reduced.

Our *in-vitro* and *in-vivo* data suggest that dasatinib exerts its anti-invasive effect in U87MG through an inhibition of focal contact formation and loss of integrin activation that occur following impairment of SFK and Focal Adhesion Kinase (FAK) activation. The $\alpha_V\beta_3$ integrin exists in two states: an active state that bind ligands such as the extracellular matrix proteins fibrinogen and fibronectin, and an inactive state that has a much lower affinity for these proteins and peptides^{23,24}. Integrin activation also affects binding of synthetic ligands, such as cyclic RGD peptides²⁴. When integrins are mobilized to the cell surface and become activated, they group in clusters known as focal adhesions with a variety of other intracellular proteins. Focal adhesions form the interface between the extracellular matrix, cell surface integrins, and the cytoskeleton. These dynamic groups of structural and regulatory proteins also transduce external signals to the cell interior²⁴. The effect of SFK on integrin-dependent invasion is mediated through FAK, which recruits other focal contact proteins or their regulators that dictate the assembly or disassembly of focal contacts and lead to cell migration^{25,26}.

In our *in-vitro* experiments dasatinib inhibited SFK and FAK at nanomolar concentrations. Furthermore, cell surface distribution of the $\alpha_V\beta_3$ integrin was drastically changed with dasatinib treatment. While in untreated cells the $\alpha_V\beta_3$ integrin was clustered in focal adhesions, the cell surface stained much more diffusely for the $\alpha_V\beta_3$ integrin following dasatinib therapy. In contrast, dasatinib did not measurably affect the total protein levels of the $\alpha_V\beta_3$ integrin or the amount of the $\alpha_V\beta_3$ integrin on the cell surface. Thus alterations in integrin clustering and activation, as opposed to a decrease in protein levels, appear to be the result of SFK/FAK inhibition.

Our *in-vivo* data are also consistent with the hypothesis that dasatinib interferes with integrin activation and thereby reduces uptake of [⁶⁴Cu]DOTA–c(RGDfK). At the time of PET imaging treated xenografts were identical in size to vehicle treated tumors and there was no evidence for treatment induced necrosis on histopathologic analysis. Moreover, a significant reduction in the tumor vasculature or integrin expression was not observed. Thus, the drastically reduced uptake of [⁶⁴Cu]DOTA–c(RGDfK) in treated xenografts cannot be explained by tumor cell death, a reduction in tumor perfusion, or a reduction in integrin expression. However, as suggested by the *in-vitro* data, dasatinib appears to decrease integrin activation resulting in decreased binding of [⁶⁴Cu]DOTA–c(RGDfK).

In conclusion, our study indicates that PET imaging with radiolabeled RGD peptides represents a novel approach for imaging *in-vivo* changes in tumor cell invasiveness in response to dasatinib. In contrast to existing techniques, PET allows longitudinal non-invasive studies that are of great interest for clinical trials, especially in diseases such as glioblastoma where serial biopsies are challenging or impossible for ethical reasons. PET imaging with RGD peptides has already been successfully used clinically to image the $\alpha_v\beta_3$ integrin in a variety of malignant tumors^{10,11}. Therefore, it will be straightforward to test our preclinical findings on monitoring dasatinib therapy with PET in clinical trials. When validated clinically, PET imaging with RGD peptides could become a unique tool for non-invasive studies of the invasive and metastatic potential of $\alpha_v\beta_3$ expressing tumors in patients.

ACKNOWLEDGMENTS

Rebecca Dumont was a Howard Hughes Medical Institute Research Training Fellow from 2006–2007. We thank Dr. David Stout, Dr. Arion Chatzioannou, Antonia Luu, Waldemar Ladno and Judy Edwards at the Crump Institute for Molecular Imaging for excellent technical assistance in small animal imaging; Stephan Schwarz at the Department of Nuclear Medicine, Medical University of Innsbruck for excellent technical assistance in producing DOTA–c(RGDfK); Julie Dang, David Nathanson, Shao-Jun Zhu, and Tiffany Huang of the Mischel Laboratory for assistance with *in-vitro* experiments. Flow cytometry was done in the UCLA Flow Cytometry Core Facility that is supported by NIH awards CA-16042 and AI-28697, and by the Jonsson Comprehensive Cancer Center, the UCLA AIDS Institute, and the David Geffen School of Medicine at UCLA.

Financial Support: UCLA ICMIC (NC1P50 CA086306) grant.

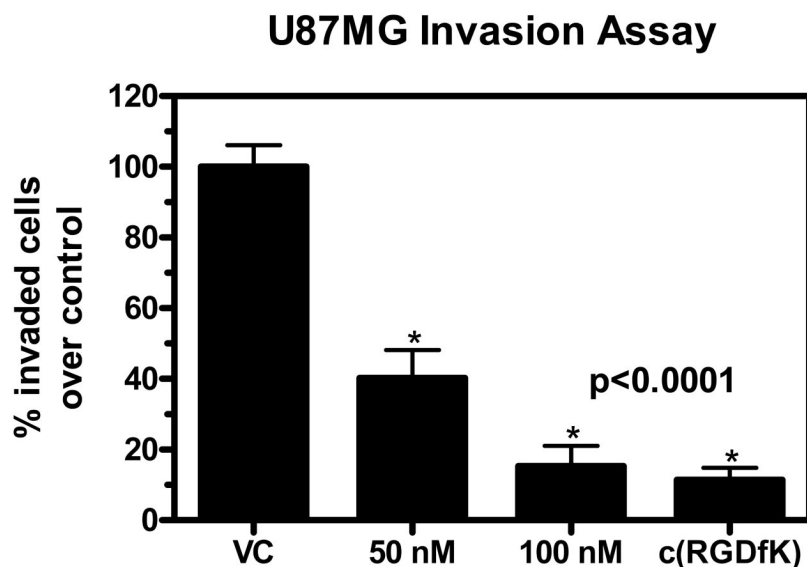
REFERENCES

1. Perez-Soler R, Chachoua A, Hammond LA, Rowinsky EK, Huberman M, Karp D, Rigas J, Clark GM, Santabarbara P, Bonomi P. Determinants of Tumor Response and Survival With Erlotinib in Patients With Non--Small-Cell Lung Cancer. *J Clin Oncol* 2004;22:3238–3247. [PubMed: 15310767]
2. Fomchenko EI, Holland EC. Platelet-derived growth factor-mediated gliomagenesis and brain tumor recruitment. *Neurosurg Clin N Am* 2007;18(viii):39–58. [PubMed: 17244553]
3. Homsy J, Cubitt C, Daud A. The Src signaling pathway: a potential target in melanoma and other malignancies. *Expert Opin Ther Targets* 2007;11:91–100. [PubMed: 17150037]
4. Macarulla T, Ramos FJ, Capdevila J, Saura C, Tabernero J. Novel targets for anticancer treatment development in colorectal cancer. *Clin Colorectal Cancer* 2006;6:265–272. [PubMed: 17241511]
5. Shor AC, Keschman EA, Lee FY, Muro-Cacho C, Letson GD, Trent JC, Pledger WJ, Jove R. Dasatinib inhibits migration and invasion in diverse human sarcoma cell lines and induces apoptosis in bone sarcoma cells dependent on SRC kinase for survival. *Cancer Res* 2007;67:2800–2808. [PubMed: 17363602]
6. Hagerstrand D, Hesselager G, Achterberg S, Wickenberg Bolin U, Kowanetz M, Kastemar M, Heldin CH, Isaksson A, Nister M, Ostman A. Characterization of an imatinib-sensitive subset of high-grade human glioma cultures. *Oncogene* 2006;25:4913–4922. [PubMed: 16547494]
7. Ding Q, Stewart J Jr, Olman MA, Klobe MR, Gladson CL. The Pattern of Enhancement of Src Kinase Activity on Platelet-derived Growth Factor Stimulation of Glioblastoma Cells Is Affected by the Integrin Engaged. *J. Biol. Chem* 2003;278:39882–39891. [PubMed: 12881526]

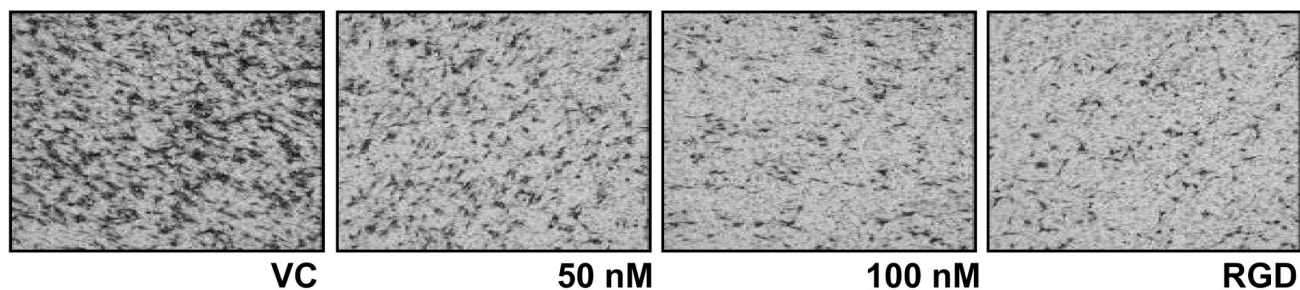
8. Hood J, Cheresh D. Role of integrins in cell invasion and migration. *Nat Rev Cancer* 2002;2:91–100. [PubMed: 12635172]
9. Haubner R, Wester H-J, Weber WA, Mang C, Ziegler SI, Goodman SL, Senekowitsch-Schmidtke R, Kessler H, Schwaiger M. Noninvasive Imaging of $\alpha v \beta 3$ Integrin Expression Using 18F-labeled RGD-containing Glycopeptide and Positron Emission Tomography. *Cancer Res* 2001;61:1781–1785. [PubMed: 11280722]
10. Haubner R, Weber WA, Beer AJ, Vabuliene E, Reim D, Sarbia M, Becker K-F, Goebel M, Heindiger, Wester H-J, Kessler H, Schwaiger M. Noninvasive Visualization of the Activated $\alpha v \beta 3$ Integrin in Cancer Patients by Positron Emission Tomography and [F18]Galacto-RGD. *PLoS Medicine* 2005;2:e70. [PubMed: 15783258]
11. Beer AJ, Haubner R, Sarbia M, Goebel M, Luderschmidt S, Grosu AL, Schnell O, Niemeyer M, Kessler H, Wester H-J, Weber WA, Schwaiger M. Positron Emission Tomography Using [18F]Galacto-RGD Identifies the Level of Integrin $\alpha v \beta 3$ Expression in Man. *Clin Cancer Res* 2006;12:3942–3949. [PubMed: 16818691]
12. Kawaguchi T, Yamashita Y, Kanamori M, Endersby R, Bankiewicz KS, Baker SJ, Bergers G, Pieper RO. The PTEN/Akt Pathway Dictates the Direct $\alpha v \beta 3$ -Dependent Growth-Inhibitory Action of an Active Fragment of Tumorstatin in Glioma Cells In vitro and In vivo. *Cancer Res* 2006;66:11331–11340. [PubMed: 17145879]
13. Decristoforo C, Hernandez Gonzalez I, Carlsen J, Rupprich M, Huisman M, Virgolini I, Wester H-J, Haubner R. ^{68}Ga - and ^{111}In -labelled DOTA-RGD peptides for imaging of $\alpha v \beta 3$ integrin expression. *European Journal of Nuclear Medicine and Molecular Imaging*. 2008
14. de Wolf HK, Snel CJ, Verbaan FJ, Schiffelers RM, Hennink WE, Storm G: Effect of cationic carriers on the pharmacokinetics and tumor localization of nucleic acids after intravenous administration. *International Journal of Pharmaceutics* 2007;331:167–175. [PubMed: 17134859]
15. Su H, Bodenstern C, Dumont RA, Seimbille Y, Dubinett S, Phelps ME, Herschman H, Czernin J, Weber W. Monitoring Tumor Glucose Utilization by Positron Emission Tomography for the Prediction of Treatment Response to Epidermal Growth Factor Receptor Kinase Inhibitors. *Clin Cancer Res* 2006;12:5659–5667. [PubMed: 17020967]
16. Li, Z-b; Cai, W.; Cao, Q.; Chen, K.; Wu, Z.; He, L.; Chen, X. ^{64}Cu -Labeled Tetrameric and Octameric RGD Peptides for Small-Animal PET of Tumor $\alpha v \beta 3$ Integrin Expression. *J Nucl Med* 2007;48:1162–1171. [PubMed: 17574975]
17. Yazdi PT, Wenning LA, Murphy RM. Influence of Cellular Trafficking on Protein Synthesis Inhibition of Immunotoxins Directed against the Transferrin Receptor. *Cancer Res* 1995;55:3763–3771. [PubMed: 7641191]
18. Loening A, Gambhir S. AMIDE: a free software tool for multimodality medical image analysis. *Molecular Imaging* 2003;2:131–137. [PubMed: 14649056]
19. Zhang X, Xiong Z, Wu Y, Cai W, Tseng JR, Gambhir SS, Chen X. Quantitative PET Imaging of Tumor Integrin $\alpha v \beta 3$ Expression with 18F-FRGD2. *J Nucl Med* 2006;47:113–121. [PubMed: 16391195]
20. Felding-Habermann B, O'Toole TE, Smith JW, Fransvea E, Ruggeri ZM, Ginsberg MH, Hughes PE, Pampori N, Shattil SJ, Saven A, Mueller BM. Integrin activation controls metastasis in human breast cancer. *Proceedings of the National Academy of Sciences* 2001;98:1853–1858.
21. Nam S, Kim D, Cheng JQ, Zhang S, Lee J-H, Buettner R, Mirosevich J, Lee FY, Jove R. Action of the Src Family Kinase Inhibitor, Dasatinib (BMS-354825), on Human Prostate Cancer Cells. *Cancer Res* 2005;65:9185–9189. [PubMed: 16230377]
22. Johnson FM, Saigal B, Talpaz M, Donato NJ. Dasatinib (BMS-354825) Tyrosine Kinase Inhibitor Suppresses Invasion and Induces Cell Cycle Arrest and Apoptosis of Head and Neck Squamous Cell Carcinoma and Non-Small Cell Lung Cancer Cells. *Clin Cancer Res* 2005;11:6924–6932. [PubMed: 16203784]
23. Kiosses WB, Shattil SJ, Pampori N, Schwartz MA. Rac recruits high-affinity integrin $\alpha v \beta 3$ to lamellipodia in endothelial cell migration. *Nat Cell Biol* 2001;3:316–320. [PubMed: 11231584]
24. Takagi J, Petre B, Walz T, Springer T. Global Conformational Rearrangements in Integrin Extracellular Domains in Outside-In and Inside-Out Signaling. *Cell* 2002;110:599–611. [PubMed: 12230977]

25. Mitra SK, Hanson DA, Schlaepfer DD. Focal adhesion kinase: in command and control of cell motility. *Nat Rev Mol Cell Biol* 2005;6:56–68. [PubMed: 15688067]
26. Playford MP, Schaller MD. The interplay between Src and integrins in normal and tumor biology. *Oncogene* 2004;23:7928–7946. [PubMed: 15489911]

A.



B.

**Figure 1.**

Invasion of U87MG cells through a fibronectin barrier is inhibited by 50 and 100 nM dasatinib and 2 mM c(RGDfK). Quantitation of invasion (A) is expressed as percent of vehicle control (VC) and was performed by calculating area stained with cresyl violet, representing cells that successfully invade through the extracellular matrix barrier. Samples performed in duplicate. P value was calculated with a 1-way ANOVA. Typical examples of the density of invasive cells after treatment with various doses of dasatinib or c(RGDfK) are shown in (B) (magnification: 40 \times).

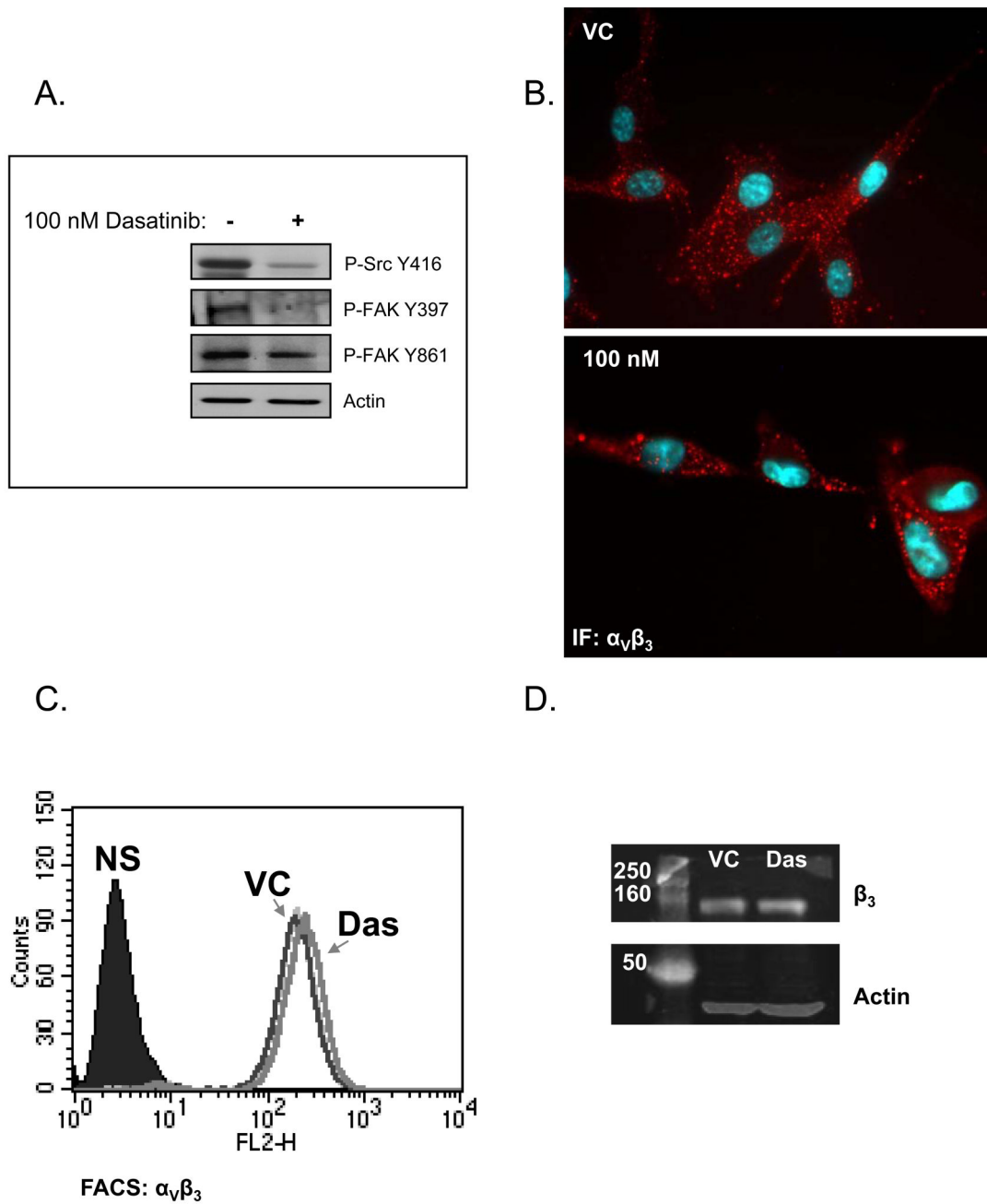


Figure 2. Western Blot of U87MG cell lysates shows target inhibition of SFK and FAK with 6 hours of 100 nM dasatinib treatment (A). Decreased formation of focal contacts in U87MG cells treated with 100 nM dasatinib for 3 hours is demonstrated by immunofluorescent staining of dimerized $\alpha_v\beta_3$ integrin (magnification: 200 \times) (B). Cell surface $\alpha_v\beta_3$ levels on FACS (C) and total β_3 protein levels on Western Blots (D) do not change with 24 hours of 100 nM dasatinib treatment. FACS samples performed in duplicate.

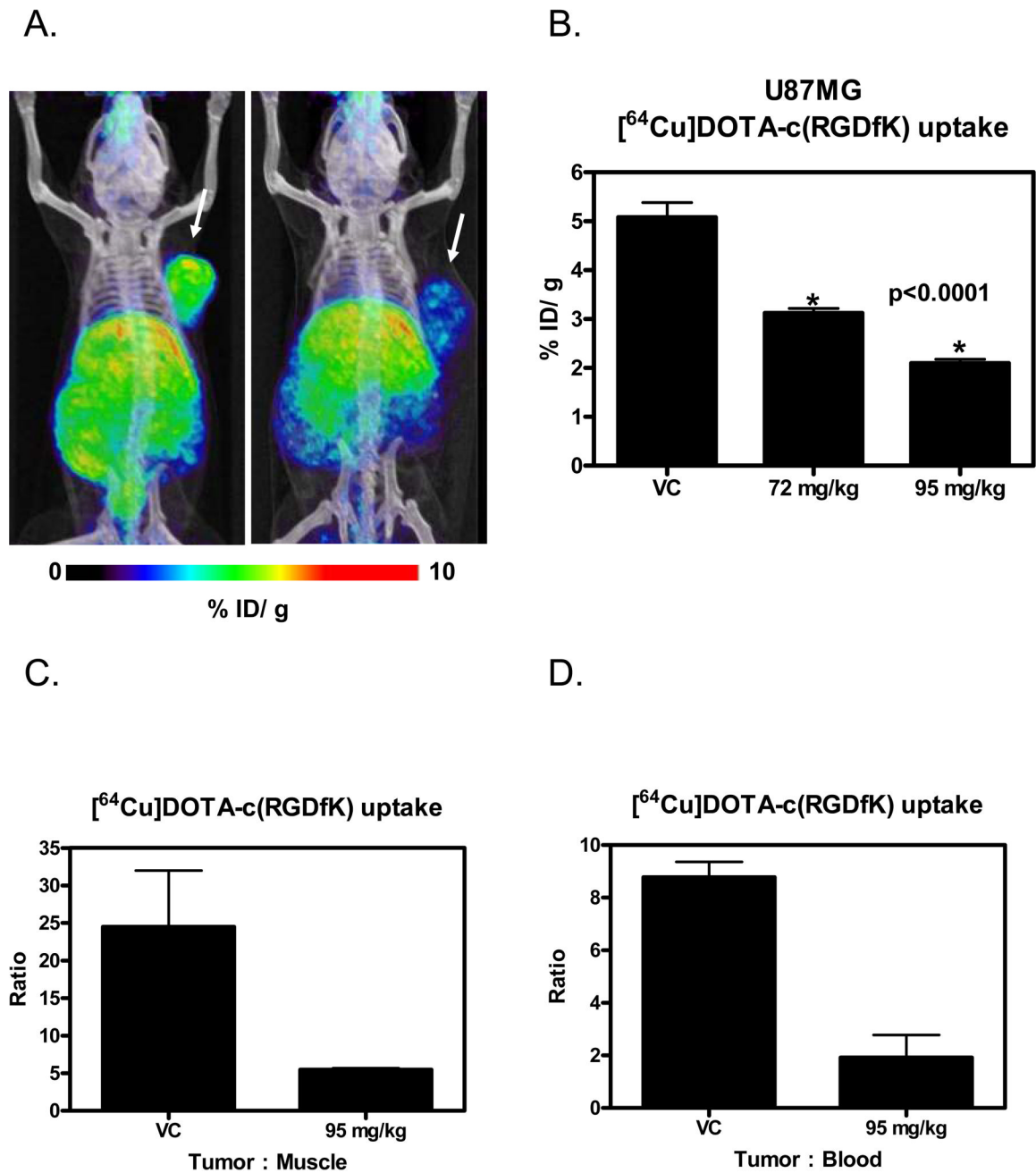


Figure 3.

Dasatinib treatment decreases U87MG uptake of [⁶⁴Cu]DOTA-c(RGDfK) *in-vivo*. (A) Maximum intensity projections of U87MG tumor bearing mice imaged with [⁶⁴Cu]DOTA-c(RGDfK), treated for 72 hours with vehicle control (left) or 95 mg/kg dasatinib (right). (B) Uptake of [⁶⁴Cu]DOTA-c(RGDfK) in U87MG xenografts after 72 hours of treatment with dasatinib or vehicle. Uptake expressed as percent injected dose/gram of tissue. P value was calculated with a 1-way ANOVA. Tumor-to-muscle (C) and tumor-to-blood ratios (D) in vehicle control and animals treated with 95 mg/kg dasatinib for 72 hours. Uptake measurements were performed 15 hours post injection of [⁶⁴Cu]DOTA-c(RGDfK).

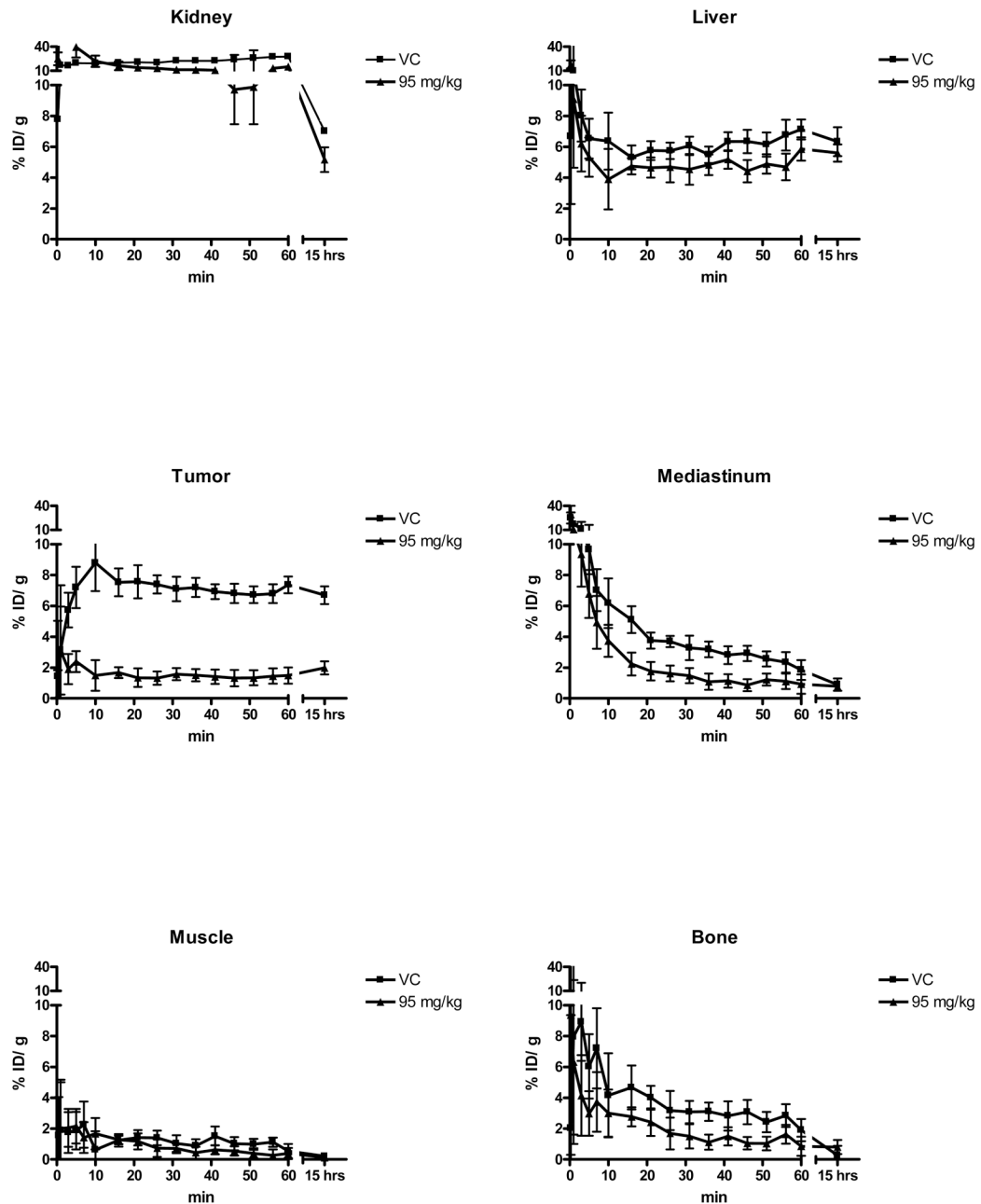


Figure 4.

Time activity curves for different organs from dynamic microPET scans following injection of $[^{64}\text{Cu}]\text{DOTA-c(RGDfK)}$ in animals treated for 72 hours with vehicle control (square) or 95 mg/kg dasatinib (triangle). The last time point represents data from 10 minute static microPET scans performed 15 hours following tracer injection. With the exception of the xenograft U87 tumor, there is no appreciable difference in tracer uptake in tissues of animals treated with dasatinib as compared to control.

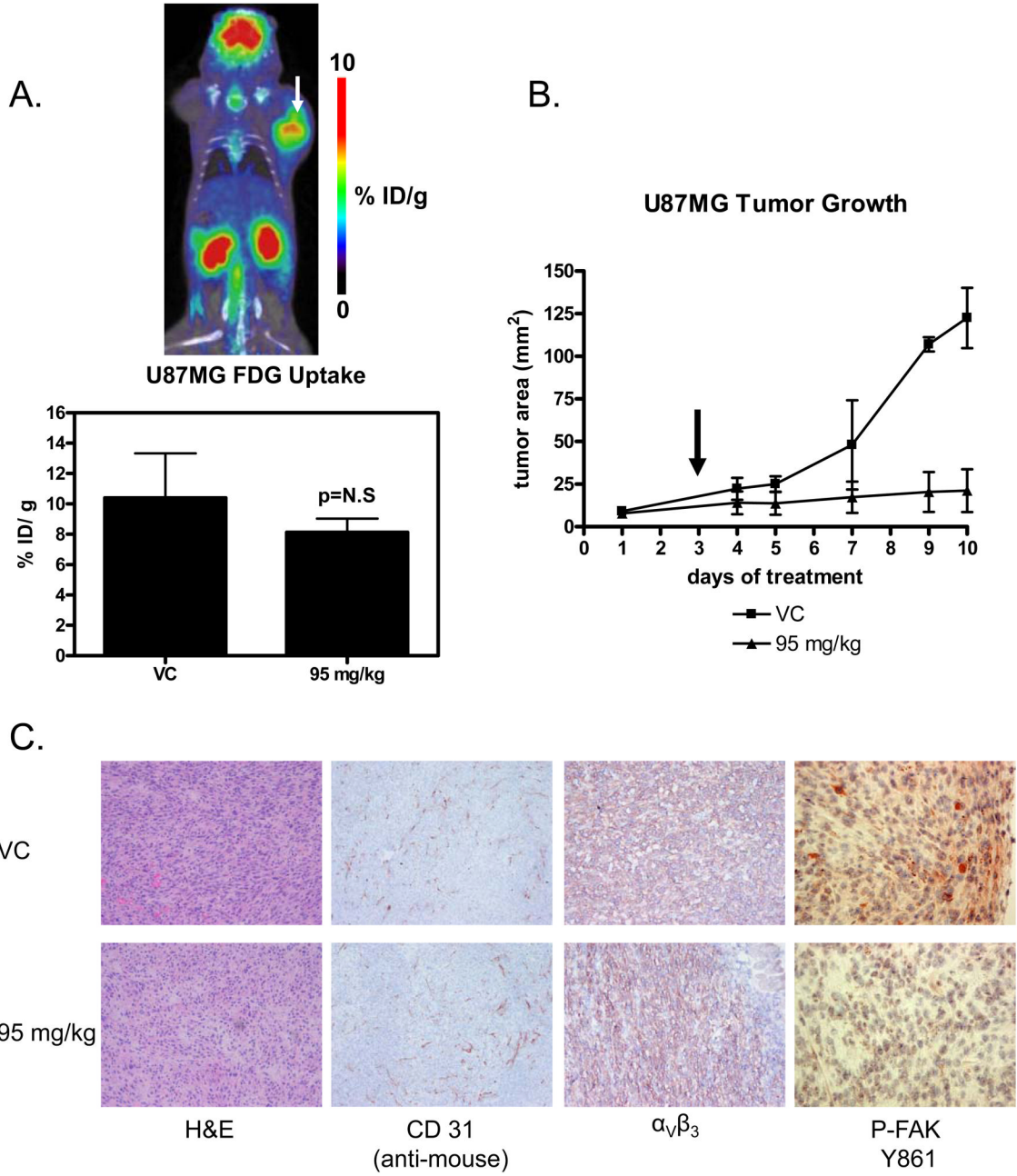


Figure 5.

(A) Coronal section of a U87MG xenograft imaged with FDG-microPET/CT after 72 hours of 95 mg/kg dasatinib and quantitation of FDG uptake expressed as percent injected dose/gram of tissue. P value was calculated with a t-test. In the image of a treated animal, a bright and globally metabolically active tumor indicates that tumors are still viable following 72 hours of 95 mg/kg dasatinib treatment. (B) U87MG xenograft tumor growth in controls and animals treated daily with 95 mg/kg dasatinib. microPET scanning was performed on day 3 (arrow). (C) Frozen sections from animals treated with control and 95 mg/kg dasatinib for 72 hours. There is no evidence of treatment induced necrosis on hematoxylin and eosin (H&E) staining or decreased vascularization (CD31 staining). In addition, $\alpha_v\beta_3$ expression on the cell surface

is unchanged with dasatinib therapy (LM609 antibody staining). Phospho-FAK is markedly decreased, demonstrating successful target inhibition by dasatinib. (magnification: 100× phospho-FAK, 40× all others).